含有(2-吡啶甲基)胺基甲基膦酸与草酸配体的同构稀土(Gd,Tb)化合物的合成、结构、磁学和荧光性质

刘美娟 曹登科* 黄 建 鲍松松 郑丽敏
(南京大学化学化工学院,配位化学国家重点实验室,南京 210093)

摘要:利用水热合成手段,(2-吡啶甲基) 胺基甲基膦酸、草酸盐与醋酸钆 (或醋酸铽) 配位组装得到 2 个同构的稀土化合物 $Ln_2(pmampH)(C_2O_4)_{2.5}(H_2O)_3\cdot 4H_2O$(Ln=Gd (**1**),Tb (**2**))。在 2 个化合物中,网状的$\{Ln_2(C_2O_4)_{2.5}\}_n$层通过$\{LnO_8\}$多面体与$\{PO_3C\}$四面体的共角连接,形成三维开放结构。沿 *b* 方向,可以观察到一维孔道,它们被未配位的(2-吡啶甲基)胺基以及晶格水分子占据。化合物 **2** 在部分或全部脱去结构中的配位以及晶格水以后,可以保持它的骨架结构。磁性研究表明化合物 **1** 表现出顺磁行为,**2** 则表现出主要的铁磁性相互作用。化合物 **2** 以及它的脱水产物的荧光性质也被测定,都表现出 Tb(Ⅲ)的特征发射,能够发出绿光。

关键词:稀土;(2-吡啶甲基)胺基甲基膦酸;草酸盐;晶体结构;磁性;荧光
中图分类号:O614.33+9;O614.341 **文献标识码**:A **文章编号**:1001-4861(2012)09-2017-08

Isostructural Lanthanide (Gd, Tb) Oxalatophosphonates with 2-Pyridylmethylamino)methyl Phosphonic Acid: Syntheses, Structures, Magnetic and Fluorescent Properties

LIU Mei-Juan CAO Deng-Ke* HUANG Jian BAO Song-Song ZHENG Li-Min
(*State Key Laboratory of Coordination Chemistry, School of Chemistry and Chemical Engineering, Nanjing University, Nanjing* 210093, *China*)

Abstract: Two isostructural lanthanide oxalatophosphonates $Ln_2(pmampH)(C_2O_4)_{2.5}(H_2O)_3\cdot 4H_2O$ (Ln=Gd (**1**), Tb (**2**)) have been obtained through hydrothermal reactions of (2-pyridylmethylamino)methyl phosphonic acid ($pmampH_2$), oxalate, and Gd/Tb salts. Both compounds exhibit 3D open framework, in which the netlike $\{Ln_2(C_2O_4)_{2.5}\}_n$ layer containing $Ln_{10}(C_2O_4)_{10}$ rings are connected through corner-sharing $\{LnO_8\}$ polyhedra and $\{PO_3C\}$ tetrahedra, generating channels along *b* axis filled with the pendant 2-pyridylmethylamino groups and lattice water molecules. The framework of **2** can be retained after partly or completely releasing coordination and lattice water molecules. The magnetic studies show that the presence of paramagnetic behavior in **1**, while dominant ferromagnetic interactions in **2**. The solid-state fluorescent measurements reveal that **2** and its dehydration products can emit green light, exhibiting characteristic transitions of Tb(Ⅲ). CCDC: 806907, **1**; 806908, **2**.

Key words: lanthanide; (2-pyridylmethylamino)methyl phosphonic acid; oxalate; crystal structure; magnetic property; fluorescent property

Lanthanide coordination polymers (LCP) have been attracting considerable interest because of their structural diversity and interesting properties such as fluorescence[1], magnetism[2], catalysis[3], etc. Organo-

收稿日期:2012-03-05。收修改稿日期:2012-05-05。
江苏省自然科学基金(No.BK2009009)和中央高校基本科研业务费(No.1106020510,1118020502)资助项目。
*通讯联系人。E-mail:dkcao@nju.edu.cn

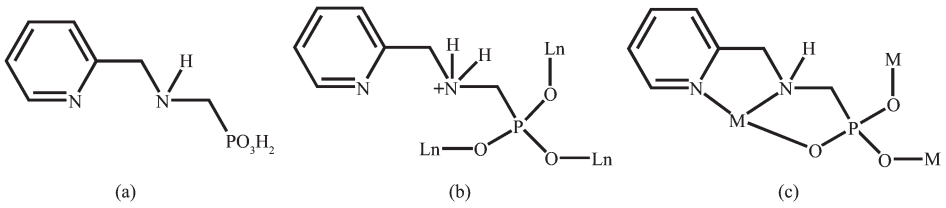

Scheme 1

phosphonate is one kind of attractive ligand for building LCP materials due to their versatile coordination modes, as well as the good thermal and chemical stabilities of the Ln-O-P bonds that phosphonate ligands made with lanthanide ions[4]. However, lanthanide phosphonates are usually poor in crystallinity, blocking the exploration of these materials. In order to overcome this problem, and also to synthesize multifunctional lanthanide phosphonates, two approaches have been commonly employed. One is the functional modification of phosphonate with organic groups, such as crown ether[5], carboxylate[6], amino[6c,7], and pyridyl[7b,8], etc. The other is the introduction of second ligand such as oxalate. It is well known that oxalate can not only mediate electronic effects between paramagnetic metal ions but also act as a linker between metal centers to yield open structures with dimensionalities ranging from zero to three[9]. So far, some lanthanide oxalatophosphonates have been reported, however, the number is still small[10-11]. Previously, we reported two chiral-layered compounds $M^{II}\{(2\text{-}C_5H_4N)CH_2NHCH_2PO_3\}(H_2O)$ (M=Mn, Cd) based on non-chiral (2-pyridylmethylamino)methyl phosphonic acid (pmampH$_2$, (2-C_5H_4N)$CH_2NHCH_2PO_3H_2$) (Scheme 1a)[12]. As an extension of our work, two isostructural Gd(Ⅲ) and Tb(Ⅲ) oxalatophosphonates incorporating pmampH$_2$ have been obtained, namely $Ln_2(pmampH)(C_2O_4)_{2.5}(H_2O)_3\cdot 4H_2O$ (Ln(Ⅲ)=Gd (**1**), Tb (**2**)). Both compounds shows 3D open framework with channels filled with the pendant 2-pyridylmethylamino groups and lattice water molecules. Their thermal stability, magnetic and fluorescent properties have been studied.

1 Experimental

1.1 Materials and physical measurements

(2-Pyridylmethylamino)methyl phosphonic acid (pmampH$_2$) was prepared according to the literature method[13]. All the other starting materials with reagent quality were obtained from commercial sources without further purification. Elemental analyses were performed with a PE 240C elemental analyzer. The infrared spectra were recorded with a VECTOR 22 spectrometer by using KBr pellets. Thermogravimetric analyses were performed with a Mettler-Toloedo TGA/DSC instrument in the temperature range 25~700 ℃ under a nitrogen flow at a heating rate of 10 ℃·min^{-1}. Powder X-ray diffraction (XRD) data were collected with a Shimadzu XRD-6000 X-ray diffractometer with Cu $K\alpha$ radiation (λ=0.154 056 nm). The fluorescence spectra were recorded on a Hitachi F-4500 spectrophotometer at room temperature, under the same measurement conditions for all samples. Magnetic susceptibility data were obtained on microcrystalline samples (2.74 mg for **1**, and 6.64 mg for **2**), using a Quantum Design MPMS-XL7 SQUID magnetometer. Diamagnetic corrections were made for both the sample holder and the compound estimated from Pascal′s constants[14].

1.2 Syntheses of $Ln_2(pmampH)(C_2O_4)_{2.5}(H_2O)_3\cdot 4H_2O$ (Ln(Ⅲ)=Gd (1), Tb (2))

Compounds **1** and **2** were synthesized following the same experimental procedure. In the typical synthesis of **1**, a mixture of pmampH$_2$ (0.10 mmol, 0.023 8 g), $Gd(CH_3CO_2)_3\cdot 6H_2O$ (0.10 mmol, 0.060 7 g), $Na_2C_2O_4$ (0.15 mmol, 0.020 1 g), and 2,2′-bipy (0.10 mmol, 0.015 6 g) in 8 mL H_2O was kept in a Teflon-lined autoclave at 120 ℃ for 7 d. After slow cooling to room temperature, colorless rod-shaped crystals were collected as a monophasic material based on the powder XRD patterns. Yield: 15 mg (34.8% based on Gd). Anal. found (calcd.) for $C_{12}H_{24}N_2O_{20}PGd_2$ (%): C,

16.74 (16.72); H, 2.81 (2.81); N, 3.37 (3.25). IR (KBr, cm^{-1}): 3 580~3 039(w, br), 2 793(w), 2 360(w), 1 669(s), 1 641(s), 1 618(m), 1 481(w), 1 437(w), 1 421(m), 1 317(w), 1 277(w), 1 154(m), 1 130(s), 1 044(m), 1 019(w), 999(m), 916(m), 792(m), 779(m), 635(w), 575(m), 492(m).

Compound **2** was obtained when $Tb(CH_3CO_2)_3\cdot 6H_2O$ was used instead of Gd $(CH_3CO_2)_3\cdot 6H_2O$. Yield: 27 mg (63.2% based on Tb). Anal. found (calcd.) for $C_{12}H_{24}N_2O_{20}PTb_2$(%): C, 16.74 (16.66); H, 2.31 (2.35); N, 2.87 (2.80). IR (KBr, cm^{-1}): 3 555~3 290 (m, br), 3 196~3 039(w, br), 2 793(w), 2 593(w), 1 670(s), 1 642(s), 1 482(w), 1 437(w), 1 317(m), 1 278(w), 1 155(m), 1 131(s), 1 047(m), 1 000(w), 917(m), 791(m), 635(w), 575(m), 493(m), 416(m).

1.3 X-ray crystallographic studies

Single crystals with dimensions 0.50 mm×0.03 mm×0.03 mm for **1**, and 0.60 mm×0.08 mm×0.06 mm for **2** were selected for structural determinations on a Bruker SMART APEX CCD diffractometer equipped with graphite monochromatized Mo $K\alpha$ radiation (λ= 0.071 073 nm) at room temperature. The data were collected in the θ range of 2.02°~25.00° for **1**, and 1.78°~25.00° for **2** by using a narrow-frame method with scan widths of 0.308° in ω and an exposure time of 10 s per frame. The numbers of the observed and unique reflections are 6 180 and 4 262 (R_{int}=0.032) for **1**, and 6 132 and 4 228 (R_{int}=0.018 4) for **2**, respectively. The data were integrated using the Siemens SAINT program[15], with the intensities corrected for Lorentz factor, polarization, air absorption, and absorption due to variation in the path length through the detector faceplate. Multi-scan absorption corrections were applied. The structures were solved by direct methods and refined on F^2 by full matrix least squares using SHELXTL[16]. All the non-hydrogen atoms were located from the Fourier maps, and were refined anisotropically. All H atoms were put in calculated positions using riding model, and were refined isotropically, with the isotropic vibration parameters related to the non-hydrogen atom to which they are bonded. The crystallographic data for **1** and **2** are listed in Table 1, and selected bond lengths are given in Tables 2.

CCDC: 806907, **1**; 806908, **2**.

Table 1　Crystallographic data for 1 and 2

Compound	**1**	**2**
Empirical formula	$C_{12}H_{24}N_2O_{20}PGd_2$	$C_{12}H_{24}N_2O_{20}PTb_2$
Formular weight	861.8	865.14
Crystal system	Triclinic	Triclinic
Space group	$P\bar{1}$	$P\bar{1}$
a / nm	1.056 68(19)	1.054 23(16)
b / nm	1.073 62(18)	1.072 33(16)
c / nm	1.180 5(2)	1.174 77(18)
α / (°)	93.099(4)	92.925(3)
β / (°)	101.692(3)	101.766(3)
γ / (°)	109.006(3)	108.851(2)
V / nm^3	1.229 5(4)	1.220 6(3)
Z	2	2
D_c / ($g\cdot cm^{-3}$)	2.328	2.354
F(000)	826	830
R_{int}	0.032 8	0.018 4
Goodness-of-fit on F^2	1.03	1.031
R_1, wR_2 ($I\geqslant 2\sigma(I)$)	0.041 4, 0.078 5	0.030 6, 0.079 5
R_1, wR_2 (All data)	0.059 7, 0.083 0	0.037 3, 0.081 8
$(\Delta\rho)_{max}$, $(\Delta\rho)_{min}$ / ($e\cdot nm^{-3}$)	1 222, −858	1 112, −823

Table 2 Selected bond lengths (nm) for 1 and 2

1					
Gd1-O1	0.224 7(5)	Gd1-O9B	0.241 0(6)	Gd2-O11D	0.242 0(5)
Gd1-O4	0.246 9(6)	Gd2-O3C	0.220 4(5)	Gd2-O13E	0.243 9(5)
Gd1-O6	0.241 4(6)	Gd2-O5	0.242 5(6)	P1-O1	0.150 8(6)
Gd1-O8	0.248 1(5)	Gd2-O7	0.241 0(5)	P1-O2	0.150 4(6)
Gd1-O1W	0.252 3(6)	Gd2-O10	0.243 1(6)	P1-O3	0.150 4(5)
Gd1-O2W	0.247 4(6)	Gd2-O12	0.240 3(5)		
Gd1-O2A	0.223 4(6)	Gd2-O3W	0.241 3(6)		
2					
Tb1-O1	0.222 9(4)	Tb1-O9B	0.240 8(4)	Tb2-O11D	0.239 0(4)
Tb1-O4	0.245 3(4)	Tb2-O5	0.242 3(4)	Tb2-O13E	0.243 9(4)
Tb1-O6	0.239 8(4)	Tb2-O7	0.239 5(4)	P1-O1	0.150 3(4)
Tb1-O8	0.246 7(4)	Tb2-O10	0.242 0(4)	P1-O2	0.150 4(4)
Tb1-O2W	0.246 0(4)	Tb2-O12	0.240 2(4)	P1-O3	0.150 4(4)
Tb1-O1W	0.250 7(4)	Tb2-O3W	0.239 5(4)		
Tb1-O2A	0.221 9(4)	Tb2-O3C	0.219 0(4)		

Symmetry codes: **1**: A: $-x+1, -y, -z+1$; B: $-x, -y, -z+1$; C: $-x+1, -y+1, -z+1$; D: $-x, -y+1, -z+1$; E: $-x, -y+1, -z$; **2**: A: $-x+1, -y, -z+1$; B: $-x, -y, -z+1$; C: $-x+1, -y+1, -z+1$; D: $-x, -y+1, -z+1$; E: $-x, -y+1, -z$.

2 Results and discussion

2.1 Syntheses

Compounds **1** and **2** were prepared through hydrothermal reactions of pmampH$_2$, $Na_2C_2O_4$, and corresponding metal acetate at 120 ℃ for 7 d. It was found that the Ln/phosphonate/oxalate molar ratio plays a key role in forming the pure phases of both compounds. The starting materials with the Ln/phosphonate/oxalate molar ratio as shown in molecular formula (1∶0.5∶1.25) always result in a mixture of single-crystal product and some powder impurities. Finally, the pure phases of **1** and **2** could be prepared using the ratio of 1∶1∶1.5. In addition, the yield of **1** is far lower that of **2** under the same experimental condition. However, the reason is not clear.

2.2 Crystal structures of 1 and 2

Compounds **1** crystallizes in triclinic space group $P\bar{1}$. The building unit consists of two unique Gd atoms, one pmampH^{2-} ligand, two and a half oxalate anions, three coordination and four lattice water molecules. As shown in Fig.1, both Gd1 and Gd2 atoms are eight-coordinated. Around Gd1, eight positions are occupied by two phosphonate oxygen atoms (O1, O2A) from two equivalent pmampH$^-$ ligands, four oxygen atoms (O4, O6, O8, O9B) from two oxalate anions, and two coordination water molecules (O1W, O2W). The Gd2 atom is surrounded by six oxygen atoms (O5, O7, O10, O11D, O12, O13E) from three oxalate anions, one phosphonate oxygen (O3C) and one water molecule (O3W). The Gd-O bond lengths and O-Gd-O bond angles fall in the range of 0.220 4(5)~0.252 3(6) nm and 66.13(18)°~150.6(2)°, respectively, comparable to those in Gd oxalatophosphonates[10a,10e].

In **1**, each oxalate anion serves as a tetra-dentate ligand using its two pairs of oxygen atoms to chelate

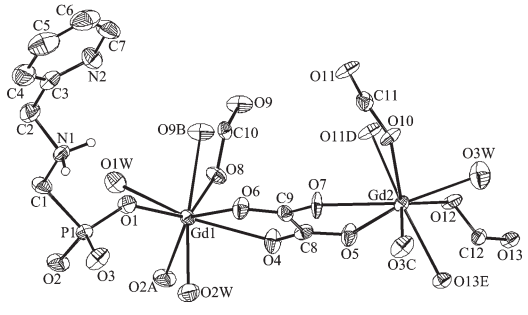

Lattice water molecules and all H atoms except those attached to the N1 atom are omitted for clarity: Symmetry codes: A: $-x+1, -y, -z+1$; B: $-x, -y, -z+1$; C: $-x+1, -y+1, -z+1$; D: $-x, -y+1, -z+1$; E: $-x, -y+1, -z$

Fig.1 Building unit of **1** with the atomic labeling scheme with 50% probability

and bridge Gd atoms into a netlike layer of $\{Gd_2(C_2O_4)_{2.5}\}_n$ containing 40-membered rings of $Gd_{10}(C_2O_4)_{10}$ (Fig.2). The similar layer was observed in compounds $[Ln_4(ox)_5(2\text{-pmpH})_2(H_2O)_7]\cdot 5H_2O$ (Ln(Ⅲ)=Gd, Tb) and $[Ln_4(ox)_5(2\text{-pmpH})_2(H_2O)_6]\cdot 6H_2O$ (Ln(Ⅲ)=Ho, Yb) (2-pmpH$_2$=2-pyridylmethylphosphonicacid)[10e]. The pmampH$^-$ ligand acts as a tri-dentate lignad, using three phosphonate oxygen atoms to bridge three Gd atoms, respectively (Scheme 1b), different from the coordination mode observed in compounds $M^{Ⅱ}\{(2\text{-}C_5H_4N)CH_2NHCH_2PO_3\}(H_2O)$ (M=Mn, Cd) (Scheme 1c)[12]. The $\{Gd_2(C_2O_4)_{2.5}\}_n$ layers are thus linked by -PO_3 groups into a 3D open framework with channels along *b* axis, in which $\{GdO_8\}$ polyhedra are corner-sharing connected through $\{PO_3C\}$ tetrahedra (Fig.3). The similar framework was founded in $[Ln_4(ox)_5(2\text{-pmpH})_2(H_2O)_6]\cdot 6H_2O$ (Ln(Ⅲ)=Ho, Yb)[10e]. However, the channels in the former are filled with 2-pyridylmethylamino groups, while pyridyl groups in the latter.

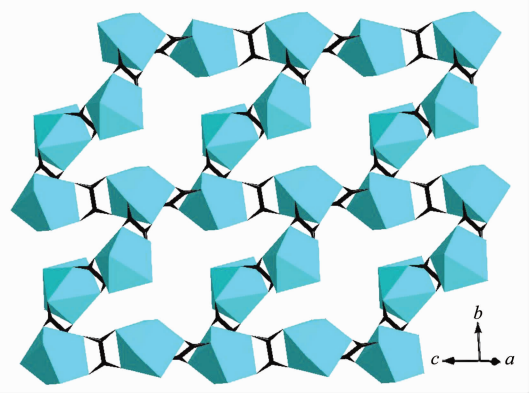

Fig.2　Netlike $\{Gd_2(C_2O_4)_{2.5}\}_n$ layer containing $Gd_{10}(C_2O_4)_{10}$ rings in **1**

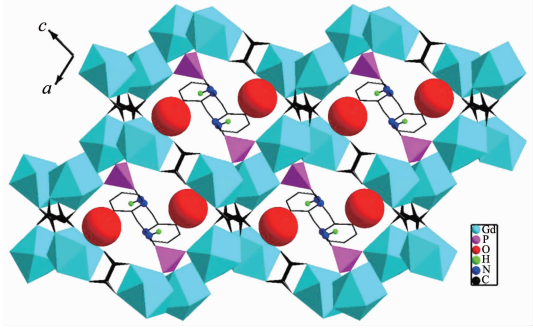

Fig.3　3D open framework of **1** resulted from the connections of $\{Gd_2(C_2O_4)_{2.5}\}_n$ layer and phosphonate groups

Compound **2** is isostructural to **1**. The Tb-O distances and O-Tb-O bond angles are in the range of 0.219 0(4)~0.250 7(4) nm and 66.45(14)°~149.74(15)°, respectively. The cell volume of **2** is smaller than that of 1 due to lanthanide contraction.

2.3　Thermal analyses

Compound **1** has a weight loss of 14.3% in the range of 52~302 ℃, corresponding to three coordination and four lattice water molecules (calcd. 14.6%). The weight loss above 302 ℃ is attributed to the decomposition of organic ligand and the collapse of structure. The TG curve of **2** is slightly different from that of **1**, although both compounds are isostructural. Compound **2** shows a weight loss of 12.2% in the temperature range of 46~120 ℃, corresponding to the release of two coordination and four lattice water molecules (calcd. 12.5%). The weight loss (2.2%) in the temperature range of 165~265 ℃ is due to the release of the last coordination water molecule (calcd. 2.1%). Above 305 ℃, compound **2** appears the decomposition of organic ligand and the collapse of structure. It should be noted that the TG curve of **2** show two clear plateaus in the temperature ranges of *ca.* 120~165 ℃ and *ca.* 265~305 ℃, respectively. Thus, compound **2** was heated under a nitrogen flow at 120 and 265 ℃, respectively, obtaining corresponding dehydrated products, namely $Tb_2(pmampH)(C_2O_4)_{2.5}H_2O$ (2*de-a*) and $Tb_2(pmampH)(C_2O_4)_{2.5}$ (2*de-b*), respectively. The powder XRD patterens indicate that the framework of **2** could be retained after dehydration treatment (Fig.4). Moreover, after a rehydration treatment by immersing samples in water at room temperature for one day, 2*de-a* and 2*de-b* can go back to the phase before dehydration, which is confirmed by powder XRD patterens (Fig.4).

2.4　Magnetic properties

The temperature-dependent magnetic susceptibilities of **1** and **2** were investigated in the temperature range of 2~300 K at the magnetic field of 1 000 Oe. For **1**, the $\chi_M T$ value at 300 K is 7.82 $cm^3\cdot K\cdot mol^{-1}$, close to the value of 7.88 $cm^3\cdot K\cdot mol^{-1}$ for one uncoupled Gd(Ⅲ) ion (S=7/2). As shown in Fig.5, the $\chi_M T$ value almost remains a constant of 7.82 $cm^3\cdot K\cdot mol^{-1}$ between 300 K and 90 K, and then decreases to

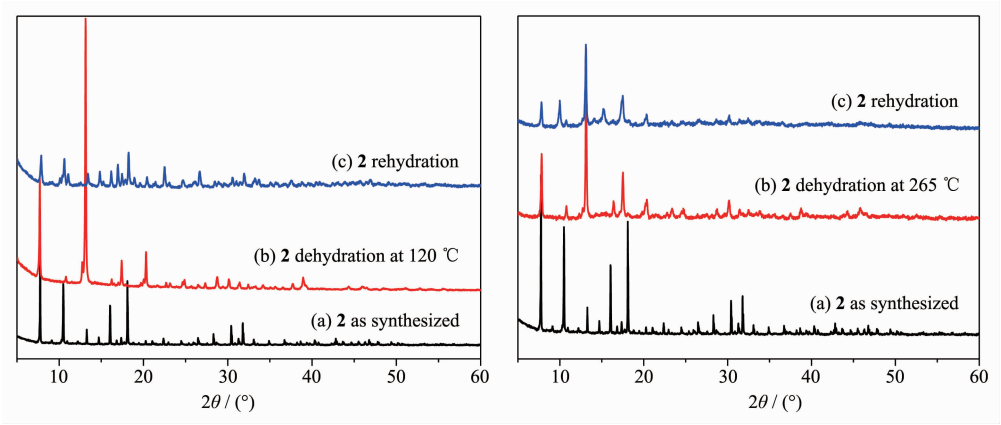

Fig.4 XRD patterns for **2**, dehydration products of **2** (at 120 ℃ and 265 ℃) and rehydration products

7.30 K·cm^3·mol^{-1} at 1.8 K. This suggests the presence of paramagnetic behavior in **1**, which is further confirmed by a small Weiss constant θ=−0.097 K.

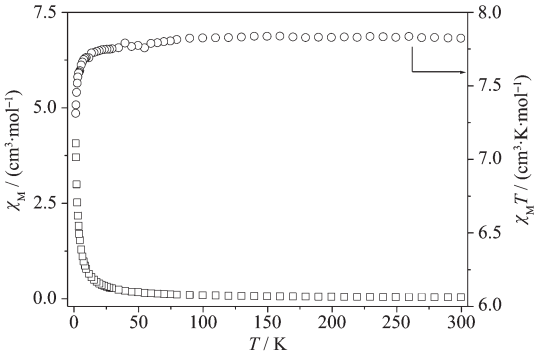

Fig.5 χ_M and χ_MT vs T curves for **1**

The magnetic behavior of **2** is quite from that of **1**, although they are isostructural. As shown in Fig.6, the χ_MT value at 300 K is 11.96 cm^3·K·mol^{-1}, close to 11.82 cm^3·K·mol^{-1} for one uncoupled Tb(Ⅲ) ion (J=6, g=3/2)[17]. Upon cooling, the χ_MT value gradually increases to 12.72 cm^3·K·mol^{-1} at 60 K, and then rapidly decreases to 9.17 cm^3·K·mol^{-1} at 1.8 K. The increase in χ_MT above 60 K indicates the presence of ferromagnetic interactions, which is further confirmed by a positive Weiss constant (θ=+8.61 K) determined in the temperature range of 100~300 K. The decrease in χ_MT below 60 K should be mainly due to the depopulation of the Stark levels[18]. The similar χ_MT vs T curves were also observed in {[Tb$_2$(Hpimda)$_2$(μ_4-C$_2$O$_4$)2H$_2$O]·4H$_2$O}$_n$ (H$_3$pimda=2-propyl-1*H*-imidazole-4,5-dicarboxylic acid) and {[Tb$_2$(dpa)$_2$(C$_2$O$_4$)$_2$(H$_2$O)$_2$]$_3$(H$_2$O)}$_n$ (dpa=2,2′-(2-methylbenzimidazolium-1,3-diyl) diacetate) where Tb (Ⅲ) ions are bridged through carboxylate and/or oxalate units, showing dominant ferromagnetic interactions[19]. The field-dependent magnetization measured at 1.8 K shows the magnetization of 5.56$N\beta$ at 70 kOe, less than expected value of 9.0 $N\beta$ for one isolated Tb(Ⅲ) ion (J=6, g=3/2).

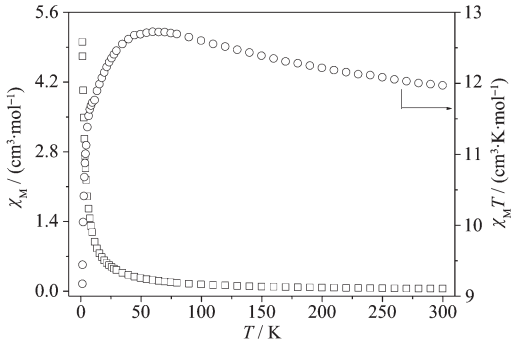

Fig.6 χ_M and χ_MT vs T curves for **2**

2.5 Fluorescent properties

The solid-state fluorescent properties of **2** and its dehydration products (2*de*-*a* and 2*de*-*b*) were investigated at room temperature under the excitation of 372 nm. As shown in Fig.7, three compounds can emit green light, showing characteristic Tb(Ⅲ) *f*-*f* transitions. Compound **2** reveals four peaks located at 375, 545, 584, and 621 nm, assigned to $^5D_4\rightarrow{}^7F_6$, $^5D_4\rightarrow{}^7F_5$, $^5D_4\rightarrow{}^7F_4$, and $^5D_4\rightarrow{}^7F_3$, respectively[20]. Among these emissions, the intensity of the $^5D_4\rightarrow{}^7F_5$ transition is the strongest one, being sensitive to the nature of the atoms that form the coordination environment[21]. Both 2*de*-*a* and 2*de*-*b* exhibit the similar emissions to those in **2**. In general, water molecules are effective nonradiative relaxers to quech fluorescence due to the loss of excitedstate energy from the Ln(Ⅲ) ions through

vibrational energy of the close proximity OH oscillator[22], Thus, comparing with **2**, dehydration products 2*de-a* and 2*de-b* shows higher fluorescent intensities (especially, for $^5D_4 \rightarrow {}^7F_5$ transition), although the increase in intensity is little.

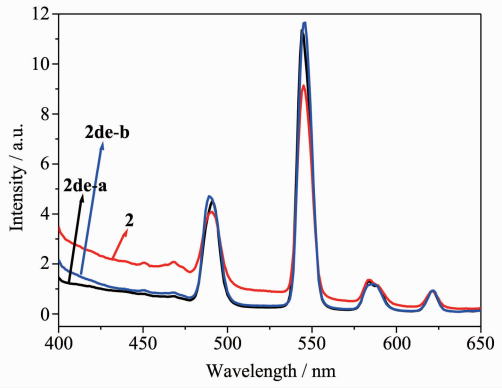

Fig.7　Emission spectra of **2** and its dehydration products upon excitation at 372 nm

3　Conclusions

This paper describes the syntheses and structures of two isostructural lanthanide oxalatophosphonates showing 3D open frameworks based on (2-pyridylmethylamino)methyl phosphonic acid ($pmampH_2$), namely, $Ln_2(pmampH)(C_2O_4)_{2.5}(H_2O)_3 \cdot 4H_2O$ (Ln=Gd (**1**), Tb (**2**)). Compound **2** shows good thermal stability, retaining its framework after partial or complete release of coordination and lattice water molecules. The paramagnetic behavior is found in **1**, while dominant ferromagnetic interactions in **2**. In the solid-state fluorescent measurements, **2** and its dehydration products exhibit typical Tb(Ⅲ) emission spectra, however, dehydration phases reveal higher fluorescent intensity.

References:

[1] (a)Bunzli J C G. *Chem. Rev.*, **2010**,**110**:2729-2755
(b)Eliseeva S V, Bunzli J C G. *Chem. Soc. Rev.*, **2010**,**39**:189-227
(c)Armelao L, Quici S, Barigelletti F, et al. *Coord. Chem. Rev.*, **2010**,**254**:487-505
(d)Tanner P A, Duan C K. *Coord. Chem. Rev.*, **2010**,**254**:3026-3029
(e)Binnemans K. *Chem. Rev.*, **2009**,**109**:4283-4374

[2] (a)Sorace L, Benellib C, Gatteschi D. *Chem. Soc. Rev.*, **2011**, **40**:3092-3104
(b)Sessoli R, Powell A K. *Coord. Chem. Rev.*, **2009**,**253**:2328-2341

[3] (a)Evans O R, Ngo H L, Lin W B. *J. Am. Chem. Soc.*, **2001**, **123**:10395-10396
(b)Aspinall H C. *Chem. Rev.*, **2002**,**102**:1807-1850
(c)Cunha-Silva L, Lima S, Ananias D, et al. *J. Mater. Chem.*, **2009**,**19**:2618-2632

[4] (a)Groves J A, Wright P A, Lightfoot P. *Inorg. Chem.*, **2005**, **44**:1736-1739
(b)Mao J G. *Coord. Chem. Rev.*, **2007**,**251**:1493-1520

[5] Ngo H L, Lin W B. *J. Am. Chem. Soc.*, **2002**,**124**:14298-14299

[6] (a)Cao D K, Hou S Z, Li Y Z, et al. *Cryst. Growth Des.*, **2009**, **9**:4445-4449
(b)Song J L, Yi F Y, Mao J G. *Cryst. Growth Des.*, **2009**,**9**:3273-3277
(c)Zhou T H, Yi F Y, Li P X, et al. *Inorg. Chem.*, **2010**,**49**:905-915

[7] (a)Liu X G, Zhou K, Dong J, et al. *Inorg. Chem.*, **2009**,**48**:1901-1905
(b)Tang S F, Song J L, Li X L, et al. *Cryst. Growth Des.*, **2007**,**7**:360-366

[8] (a)Cao D K, Li Y Z, Song Y, et al. *Inorg. Chem.*, **2005**,**44**:3599-3604
(b)Galezowska J, Janicki R, Kozlowski H, et al. *Eur. J. Inorg. Chem.*, **2010**,**11**:1696-1702

[9] (a)Rao C N R, Natarajan S, Vaidhyanathan R. *Angew. Chem. Int. Ed.*, **2004**,**43**:1466-1496, and some references therein
(b)Zhang L Z, Gu W, Li B, et al. *Inorg. Chem.*, **2007**,**46**:622-624

[10](a)Song J L, Mao J G. *Chem. Eur. J.*, **2005**,**11**:1417-1424
(b)Ying S M, Mao J G. *Cryst. Growth Des.*, **2006**,**6**:964-968
(c)Huang Y L, Huang M Y, Chan T H, et al. *Chem. Mater.*, **2007**,**19**:3232-3237
(d)Li X, Liu T, Lin Q, et al. *Cryst. Growth Des.*, **2010**,**10**:608-617
(e)Yang T H, Cao D K, Li Y Z, et al. *J. Solid State Chem.*, **2010**,**183**:1159-1164
(f)Zhang L, Xu S, Zhou Y, et al. *CrystEngComm*, **2011**,**13**:6511-6519

[11](a)Zhao Y, Li J, Sun Z G, et al. *Inorg. Chem. Commun.*, **2008**, **11**:1057-1059
(b)Zhu Y Y, Sun Z G, Zhao Y, et al. *New J. Chem.*, **2009**, **33**:119-124
(c)Zhu Y Y, Sun Z G, Chen H, et al. *Cryst. Growth Des.*, **2009**,**9**:3228-3234
(d)Liu L, Sun Z G, Zhang N, et al. *Cryst. Growth Des.*, **2010**,**10**:406-413
(e)Zhu Y Y, Sun Z G, Tong F, et al. *Dalton Trans.*, **2011**,

40:5584-5590

[12]Hou S Z, Cao D K, Li Y Z, et al. *Inorg. Chem.*, **2008**,**47**: 10211-10213

[13]Bakhmutova A E V, Bestaoui N, Bakhmutov V I, et al. *Inorg. Chem.*, **2004**,**43**:1264-1272

[14]Kahn O. *Molecular Magnetism*. New York: VCH Publishers, **1993**.

[15]*SAINT, Program for Data Extraction and Reduction, Siemens Analytical X-ray Instruments*, Madison, WI, **1994-1996**.

[16](a)*SHELXTL* (*Version* 5.0), *Reference Manual, Siemens Industrial Automation*, Analytical Instruments, Madison, WI, **1995**.

(b)Sheldrick G M, *Acta Crystallographica Section A*, **2008**, **64**:112-122

[17]Benelli C, Gatteschi D. *Chem. Rev.*, **2002**,**102**:2369-2387

[18](a)Bunzli J C G, Chopin G R. *Lanthanide Probes in Life, Chemical and Earth Sciences*. Amsterdam: Elsevier, **1989**.

(b)Costes J P, Nicodeme F. *Chem. Eur. J.*, **2002**,**8**:3442-3447

[19](a)Feng X, Zhao J, Liu B, et al. *Cryst. Growth Des.*, **2010**, **10**:1399-1408

(b)Wang X J, Cen Z M, Ni Q L, et al. *Cryst. Growth Des.*, **2010**,**10**:2960-2968

[20](a)Zhu W H, Wang Z M, Gao S. *Inorg. Chem.*, **2007**,**46**: 1337-1342

(b)Lin Z J, Xu B, Liu T F, et al. *Eur. J. Inorg. Chem.*, **2010**, 3842-3849

[21]Cepeda J, Balda R, Beobide G, et al. *Inorg. Chem.*, **2011**, **50**:8473-8451, and references therein

[22]Liu T F, Zhang W, Sun W H, et al. *Inorg. Chem.*, **2011**,**50**: 5242-5248